Journal of Power Sources 245 (2014) 684–690

Contents lists available at SciVerse ScienceDirect

Journal of Power Sources

journal homepage: www.elsevier.com/locate/jpowsour

Short communication

Stability of spinel $Li_4Ti_5O_{12}$ in air

Yurui Gao, Zhaoxiang Wang*, Liquan Chen

Key Laboratory for Renewable Energy, Beijing Key Laboratory for New Energy Materials and Devices, National Laboratory for Condensed Matter Physics, Institute of Physics, Chinese Academy of Sciences, PO Box 603, Beijing 100190, China

HIGHLIGHTS

- Li_2CO_3 is detected on $Li_4Ti_5O_{12}$ surface exposed to air.
- First-principles calculations show that $Li_4Ti_5O_{12}$ is lithium-truncated at surface.
- Surface reactions on $Li_4Ti_5O_{12}$ with H_2O and CO_2 air are suggested.
- Impact of air-exposure on electrochemical performances of $Li_4Ti_5O_{12}$ is evaluated.

GRAPHICAL ABSTRACT

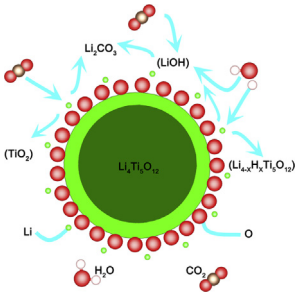

ARTICLE INFO

Article history:
Received 13 May 2013
Received in revised form
4 July 2013
Accepted 6 July 2013
Available online 15 July 2013

Keywords:
Lithium ion batteries
Stability
First-principles calculation
Surface

ABSTRACT

As a promising anode material alternative to the carbons, $Li_4Ti_5O_{12}$ has drawn wide attention for its overwhelming advantages in meeting requirements of lithium ion batteries with high power density, long cycling life and safety for electric vehicles and electricity storage stations. Its stability issue during storage is interesting and of large importance. In this work, the stability of commercial spinel $Li_4Ti_5O_{12}$ material in air has been characterized by a series of physical and electrochemical techniques. First-principles calculations indicate that $Li_4Ti_5O_{12}$ is lithium-truncated at the surface. This explains why it tends to absorb H_2O and CO_2 to form Li_2CO_3 but the formation of Li_2CO_3 does not significantly impact its electrochemical performances.

1. Introduction

Lithium-ion batteries (LIBs) that have been widely used as the major power sources for portable electronic devices are regarded as a promising candidate of power sources for electric vehicles and large-scale electricity storage stations. However, they meet challenges in high power density, long cycling life and high safety requirements in these applications [1]. Spinel $Li_4Ti_5O_{12}$ draws much interest due to its advantages such as high cycling stability and excellent rate performance [2–6]. However, as the electrode material is usually exposed to air for a time interval from a couple of weeks to one month or longer between its production and application, the structural stability of $Li_4Ti_5O_{12}$ against air or even moisture should be an interesting topic to be comprehensively investigated. This will also be beneficial to the application of $Li_4Ti_5O_{12}$.

Actually the stability issue of the Li-containing material is pervasive. Simon et al. [7] examined the stability of $Li_4Ti_5O_{12}$ in acidic solutions and observed the exchange between the proton and the lithium ions in it. They attributed the instability of $Li_4Ti_5O_{12}$ to its weakly acidic atmosphere pH. Snyder et al. [8] used diffuse reflectance infrared Fourier transform spectroscopy to study the surface chemistry of $Li_4Ti_5O_{12}$ and found the presence of Li_2CO_3 on

* Corresponding author. Tel.: +86 10 82649047; fax: +86 10 82649050.
E-mail address: zxwang@iphy.ac.cn (Z. Wang).

0378-7753/$ – see front matter © 2013 Elsevier B.V. All rights reserved.
http://dx.doi.org/10.1016/j.jpowsour.2013.07.031

it. The stability of other electrode materials has also been widely investigated. It was reported that CO_2 reacts with lithium-rich $Li_{1+z}Ni_{1-x-y}Co_xM_yO_2$ (M for Al and Mn) during storage to form Li_2CO_3 and O_2 and reduce Ni^{3+} to Ni^{2+} by a two-step reaction [9–11]. We previously studied the stability of commercial $LiFePO_4$ and found it oxidized/decomposed to Li_3PO_4, $FePO_4$ and Fe_2O_3 in air [12]. Even the Li-insufficient $Li_{0.30}La_{0.57}TiO_3$ was found to react with ambient air and form Li_2CO_3 [13]. However, these authors did not try further to understand the intrinsic reasons (from the point of the structural features of the active material) for the instability.

Since the stability of $Li_4Ti_5O_{12}$ during storage and its surface structure features are rarely touched but are of great importance if $Li_4Ti_5O_{12}$ is to be used in battery manufactory, this work is to characterize the stability of $Li_4Ti_5O_{12}$ in air, evaluate its impact on the electrochemical performances and understand the structural reason for its instability. It will be seen that Li_2CO_3 exists on the surface of air-stored commercial $Li_4Ti_5O_{12}$. Based on the experimental and first-principles calculations results, the reaction mechanism is proposed to explain the formation of Li_2CO_3 on the surface.

2. Experimental sections

2.1. Materials preparation

Commercial $Li_4Ti_5O_{12}$ (Altairnano; tap density 0.71 g cm^{-3}) that had been stored in ambient air for about one month was used in this work. For comparison, fresh $Li_4Ti_5O_{12}$ (specific surface area ~ 2 m^2 g^{-1}) was synthesized by annealing stoichiometric amounts of commercial Li_2CO_3 (2 mol % excess added to compensate for the lithium loss) and TiO_2 at 800 °C for 20 h in air. The home-prepared $Li_4Ti_5O_{12}$ was then exposed to air at room temperature for 30 days.

2.2. Physical characterization

The morphologies of the samples were investigated by scanning electron microscope (SEM, Hitachi S-4800) and transmission electron microscope (TEM, Tecnai G2 F20 U-TWIN), respectively. X-ray diffraction (XRD) patterns were obtained on an X'Pert Pro MPD X-ray diffractometer (Cu Kα1, $\lambda = 1.5418$ Å). As spinel $Li_4Ti_5O_{12}$ is well-known as a "zero-stain" lithium insertion material, the lattice changes during storage in air are expected to be rather small. Therefore, errors from the XRD diffractometer must be considered. In order to diminish these errors, the XRD patterns of $Li_4Ti_5O_{12}$ at different status were calibrated by silicon. For the recording of the Fourier Transform Infrared (FTIR) spectra, the sample powder was dispersed in dried KBr, pressed into pellet, and irradiated in the vacuum chamber of a Vertex 70v spectrometer (Bruker Optics, Germany) with a transmission mode at a resolution of 4 cm^{-1}. The content of Li_2CO_3 in the material was measured on Thermogravimetry–Differential Scanning Calorimetry (TG–DSC, NETZSCH STA409C, Germany) at a heating rate of 10 °C min^{-1} from the room temperature to 800 °C in nitrogen.

2.3. Electrochemical evaluation

Electrodes were prepared by mixing $Li_4Ti_5O_{12}$ powder, carbon black and polyvinylidene fluoride (PVDF) dissolved in *N*-methylpyrrolidone (NMP) at a weight ratio of 8:1:1 to form a homogeneous

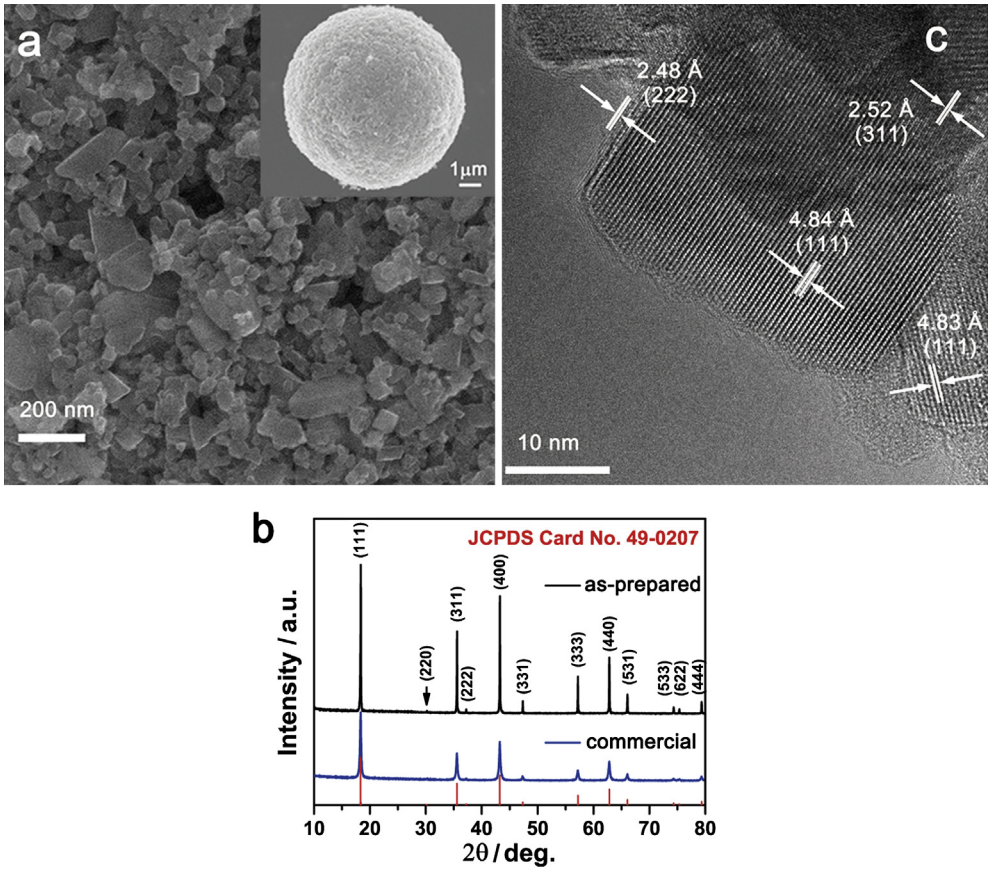

Fig. 1. The surface morphology (a) and structural features ((b) for XRD patterns and (c) for TEM image) of the commercial $Li_4Ti_5O_{12}$. The XRD pattern of the home-prepared fresh $Li_4Ti_5O_{12}$ is also shows in (b) for comparison.

slurry. The slurry was then uniformly cast onto a piece of aluminium (Al) foil as the current collector. Electrode sheets were dried in vacuum at 100 °C for 8 h. Test cells were assembled in an Ar-filled glove box (MBraun, Lab Master 130) with the fresh lithium foil as the counter electrode, Celgard 2400 as the separator, and 1 M $LiPF_6$ dissolved in ethylene carbonate and dimethyl carbonate (EC-DMC) (1:1 v/v) as the electrolyte. The half-cell was galvanostatically (dis) charged between 1.0 and 2.0 V *vs.* Li^+/Li at a current density of 17.5 mA g^{-1} on a Land BA2100A battery tester (Wuhan, China).

2.4. Calculational details

Spin-polarized calculations were carried out within the framework of density functional theory (DFT) [14,15] using pseudopotentials established by the projector-augmented wave (PAW) method [16] and the Perdew–Burke–Ernzerhof (PBE) exchange–correlation functional [17], as implemented in the Vienna Ab-initio Simulation Package (VASP) [18,19], a plane wave density functional code. A Hubbard-type correction U for Ti-3d states was taken into account [20,21]. The effective U value was set to 2.5 eV [22,23]. The cutoff energy for the plane-wave basis was 500 eV for all calculations. All of the atoms were relaxed until Hellmann–Feynman force convergence was achieved at 0.01 eV $Å^{-1}$. The simulations were performed on the 7-layers-TiO_6 model with symmetrical surfaces and the thickness of the slab was 42.18 Å separated by a 25 Å vacuum layer. A 3 × 3 × 1 Monkhorst–Pack k-mesh was used.

3. Results and discussions

3.1. Physical characterization

The typical morphology of the commercial $Li_4Ti_5O_{12}$ with a specific surface area of 38.7 $m^2\ g^{-1}$ is shown in Fig. 1a. The spherical particles are composed of nano-sized $Li_4Ti_5O_{12}$ crystallites. No impurity phases are observed in the XRD pattern (Fig. 1b). A simple calculation indicates that the cell parameter of the $Li_4Ti_5O_{12}$ is $a = 8.35$ Å, very close to the lattice parameter a value (8.358 Å) in the JCPDS card (No. 49-0207).

More structural details are observed by TEM imaging (Fig. 1c). It is seen that the lattice fringe of the $Li_4Ti_5O_{12}$ almost extends to the edge of its primary particle. The $Li_4Ti_5O_{12}$ (111) facet is often observed in the TEM field with a spacing distance of 4.84 Å, consistent with that from the XRD analysis. No amorphous species is observed on the $Li_4Ti_5O_{12}$ particle.

However, Li_2CO_3 is clearly detected in both the commercial and the home-prepared $Li_4Ti_5O_{12}$ (Fig. 2) (see Fig. 1S for the morphology of the latter). The broad and strong bands at 658 and 473 cm^{-1} in the commercial sample are assigned to the Ti–O and Li–O vibrations [24,25]. The band at 1639 cm^{-1} is attributed to the bending of the adsorbed water [26,27]. Compared with the FTIR spectrum of commercial Li_2CO_3 and as-prepared Li_2O (obtained by heating commercial Li_2CO_3 in air at 900 °C for 16 h) (Fig. 2b), the strong peaks at 1503 and 1444 cm^{-1} (asymmetric CO stretching), the sharp peak at 1385 cm^{-1} (symmetric CO stretching) and the weak peak at

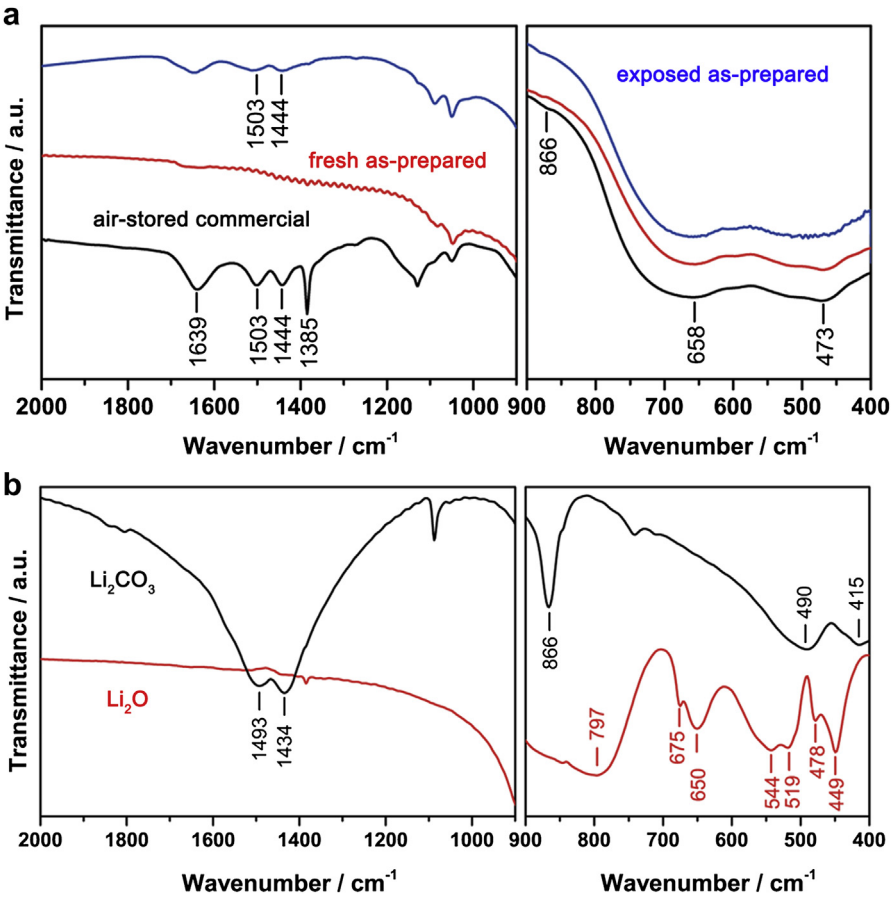

Fig. 2. FTIR spectra of the air-stored commercial $Li_4Ti_5O_{12}$, fresh and air-exposed (30 days at room temperature) home-prepared $Li_4Ti_5O_{12}$ (a). FTIR spectra of the commercial Li_2CO_3 and as-prepared Li_2O are shown in (b) for comparison.

866 cm^{-1} (out-of-plane bending of the carbonate) are attributed to the Li_2CO_3 [28,29] (See Figs. 2S and 3S for further evidence that these peaks should not be attributed to Ti-containing carbonates). The position difference of the same modes in the FTIR spectrum of the commercial $Li_4Ti_5O_{12}$ and in that of the commercial Li_2CO_3 is due to the different environments where the Li_2CO_3 is located. That is, the Ti–O octahedrons affect the CO_3^{2-} vibration. Li_2CO_3 is also recognized in the home-prepared $Li_4Ti_5O_{12}$ that has been exposed to air at room temperature for 30 days (Fig. 2a). The discrepancy between the FTIR and the XRD or TEM is attributed to the amorphous feature of the Li_2CO_3, its low content or even inhomogeneous distribution on the surface of $Li_4Ti_5O_{12}$ as well as the higher detection sensitivity of FTIR spectroscopy than that of the XRD and TEM techniques. These results also indicate that the formation of Li_2CO_3 on the surface of $Li_4Ti_5O_{12}$ does not affect its bulk structure.

3.2. Density functional theory (DFT) calculations

First-principles calculations were performed to understand the preferential formation of Li_2CO_3 on the surface of $Li_4Ti_5O_{12}$. As the surface of $Li_4Ti_5O_{12}$ contains complex conditions induced by the 16d-site lithium atoms, we seek another simple way to reach the surface of $Li_4Ti_5O_{12}$. As spinel $Li_4Ti_5O_{12}$ (or written as $[Li_3]_{8a}[LiTi_5]_{16d}[O_{12}]_{32e}$) [2,30] can be regarded as a defective spinel $LiTi_2O_4$ ($[Li]_{8a}[Ti_2]_{16d}[O_4]_{32e}$), $LiTi_2O_4$ is hereby taken as the model to investigate the surface structural features of $Li_4Ti_5O_{12}$. The difference due to such simplification will be discussed later in this article.

Clearly there exist various facets at the surface of spinel $Li_4Ti_5O_{12}$. The (111) facet is chosen for the following calculations because it shows the strongest diffraction intensity in the XRD patterns and is often observed in the TEM image (Fig. 1c).

The number of the broken Ti–O bonds at the surface is first explored. Fig. 3 shows the initial model. For easy description, the 8a site at the outmost surface is denoted as 8a-m, the 16c site at the outmost surface as 16c-m, the 8a site next to the outmost surface as 8a-n and the 16c site next to the outmost surface as 16c-n. By simultaneously removing the oxygen atoms on the top and at the bottom surfaces in the TiO_6 octahedron, the number of the Ti–O bonds can be changed. The formation energy of the Ti–O bonds at the surface is defined as

$$E_{f-x} = \left(E_{\mathrm{LTO}(-x)} - E_{\mathrm{LTO(no)}} + xE_{\mathrm{O_2}}\right)/2,$$

where $E_{\mathrm{LTO}(-x)}$ is the free energy of the system in which x couples of oxygen atoms are removed from the surface, $E_{\mathrm{LTO(no)}}$ is the free energy of the initial system in which no Ti–O bond is broken at the surface, and $E_{\mathrm{O_2}}$ is the free energy of O_2. For the formation energy of x Ti–O bonds broken at the surface, E_{f-x}, the counterpart inside the parenthesis is supposed to be divided by 2.

Fig. 4 shows the formation energy of the broken Ti–O bonds. The formation energy is 4.12 eV when the first Ti–O bond is broken. As more Ti–O bonds are broken, the formation energy increases linearly. Considering the initial condition that the formation energy is zero when no Ti–O bond is broken,

$$E_{f-x}(x = 0) = 0,$$

a linear relationship can be built as

$$E_{f-x} = kx,$$

where the slope k equals to 4.703 eV according the results of least square fitting. This value approximately represents the energy of one Ti–O bond at the surface. This explains why the Ti–O bond at the surface is difficult to be broken, due to the strong Ti–O covalent interaction. Therefore, a surface with none of the Ti–O bonds broken is assumed in the following discussion.

Based on the supposal that the Ti–O bonds are not broken at the surface, the truncating plane can only be placed in two possible positions (Fig. 3). Case 1 corresponds to the above case where no Ti–O bonds are broken at the surface (the initial model). In case 2, the lithium atoms occupy the 8a-m site; the surface is truncated with lithium atoms. We will discuss this case in detail hereinafter.

Firstly, the lithium atom is placed at the 8a-m site (Fig. 5a) based on the initial structure. Upon relaxed, it migrates close to the 16c-m site (Fig. 5b), corresponding to formation energy of

$$E_{\mathrm{formation}} = \left(E_{\mathrm{LTO(16c)}} - E_{\mathrm{LTO(no)}} - 2E_{\mathrm{Li}}\right)/2,$$

where $E_{\mathrm{LTO(no)}}$ is the free energy of the initial system in which no lithium atoms occupy the 16c-m site or the 8a-m site (Fig. 3),

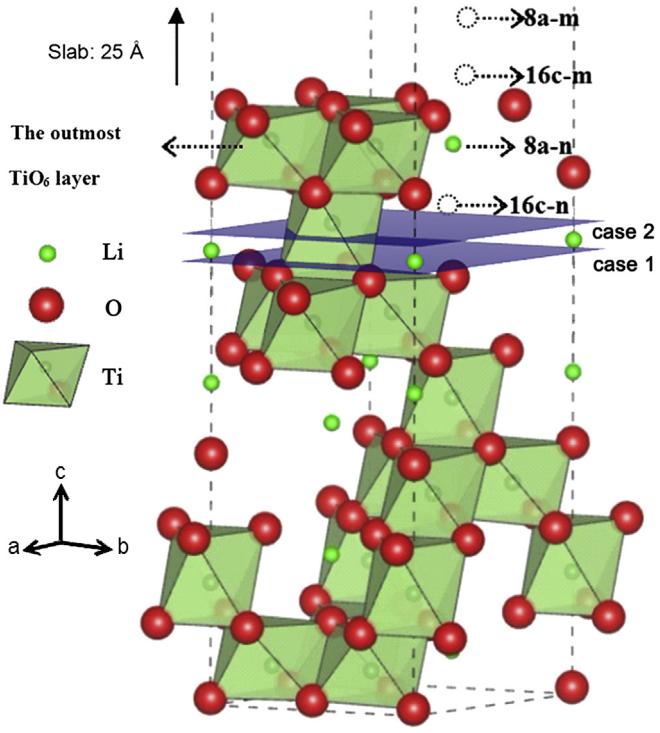

Fig. 3. The initial system of $LiTi_2O_4$ (111) surface: 8a-m (8a site at the outmost surface); 16c-m (16c site at the outmost surface); 8a-n (8a site next to the outmost surface); 16c-n (16c site next to the outmost surface). The 8a-m, 16-m and 16c-n sites are not occupied in the initial model. Case 1 and case 2 sketch two possible truncating planes considering the supposal that Ti–O bonds are unbroken at the surface.

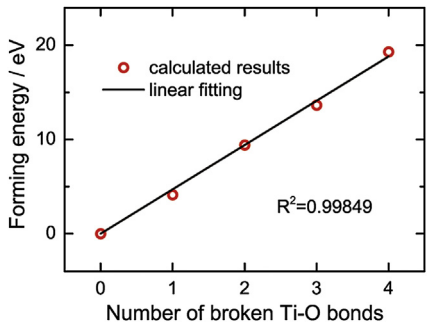

Fig. 4. Dependence of the formation energy on the number of the broken Ti–O bonds at the surface. Entropy is not considered.

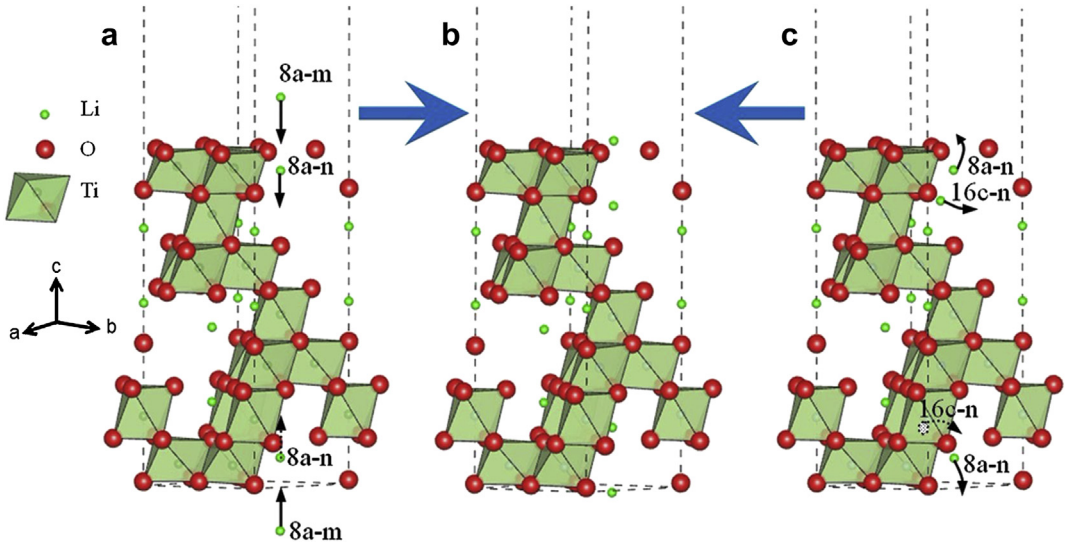

Fig. 5. Scheme for the migration route of the Li atoms on the 8a-m site (a) and the Li atom on the 16c-n site (c) towards the 16c-m site (b).

$E_{LTO(16c)}$ is the free energy of the system in which lithium atoms symmetrically occupy the 16c-m site (Fig. 5b), and E_{Li} is the free energy of the metallic lithium. The formation energy of one lithium atom occupying the 16c-m site is calculated to be −2.92 eV. That is, the lithium atoms prefer to occupy the 16c-m site which is at the outmost surface. This is true even if the lithium atom is originally located at the 16c-n site rather than at the 16c-m site (Fig. 5c). In this case, the lithium atom at the 16c-n site will expel the lithium atom on the 8a-n site to the 16c-m site while the 16c-n lithium moves closer to the 8a-n site from which the original lithium leaves (Fig. 5b).

Secondly, with the 16c-m site occupied by lithium atom, we suppose that the 16c-n site is also occupied by the lithium atoms so as to calculate the formation energy for a lithium-rich surface (Fig. 6). The formation energy for the lithium atom on the 16c-n site is defined as

$$E_{\text{formation}} = \left(E_{LTO(16c-16c)} - E_{LTO(16c)} - 2E_{Li}\right)/2,$$

where $E_{LTO(16c-16c)}$ is the free energy of the system in which lithium atoms occupy both the 16c-n site and the 16c-m site shown in Fig. 6b. The formation energy is calculated to be −0.97 eV, approximate to the formation energy of lithium insertion into the $LiTi_2O_4$ bulk, meaning that excess Li-ions arrangement in the inner layers will not be affected by the environment outside the TiO_6 layer. This further indicates that the TiO_6 layer at the outmost surface plays an important role in isolating the inner layers from the outer environment. Such a shielding effect helps to stabilize the electrochemical performances of $Li_4Ti_5O_{12}$, the lithium insertion/extraction potential plateau, for example.

Now we discuss the difference that might arise due to taking spinel $LiTi_2O_4$ for spinel $Li_4Ti_5O_{12}$ in the above calculations. The structural difference between $LiTi_2O_4$ and $Li_4Ti_5O_{12}$ lies in the fact

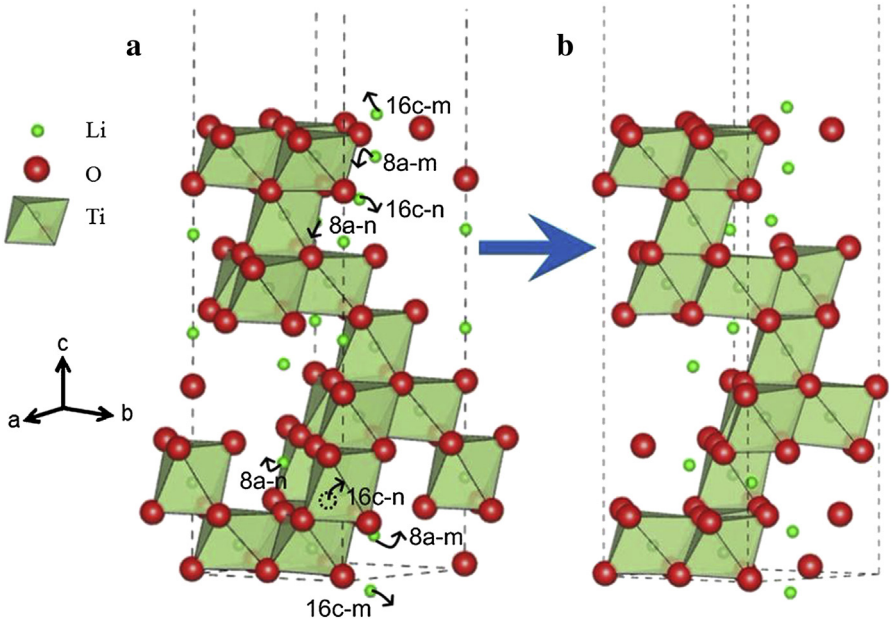

Fig. 6. Scheme for the relaxation of the Li atoms on the 16c-n site with one Li atom occupying the 16c-m site (a) and the results of the relaxation (b).

that some of the 16d sites, the Ti site in $LiTi_2O_4$, are occupied by the lithium atoms in $Li_4Ti_5O_{12}$. Such substitution will not affect the occupancy of the lithium at the surface if it occurs in the bulk. If it takes place in the TiO_6 octahedral layer close to the outmost surface, the lithium occupancy at the outmost surface will not be affected either, due to the shielding effect of the TiO_6 layer at the outmost surface. However, if this substitution occurs in the outmost TiO_6 layer, the formation energy will be higher than that when the substitution takes place in the internal part. This means that the probability of such substitution is lower to occur in the outmost TiO_6 layer. Moreover, even if the substitution occurs in the outmost TiO_6 layer, the 16c-m site that is at the outmost surface will prefer to be occupied by the lithium atom, corresponding to lower formation energy of −4.37 eV. In this case, the surface is still truncated with lithium atoms. Therefore, the error due to replacing $Li_4Ti_5O_{12}$ with $LiTi_2O_4$ for simulation is negligible.

3.3. Electrochemical evaluation

The impact of air-exposure on the electrochemical performances of $Li_4Ti_5O_{12}$ was evaluated by assembling the as-received (air-tight packed and supposed to be "fresh") and air-exposed commercial $Li_4Ti_5O_{12}$ as the working electrode of $Li/Li_4Ti_5O_{12}$ button cells, respectively (Fig. 4S). Clearly the surface chemistry of an electrode material has the most significant impact on its coulombic efficiency and initial reversible capacity. However, our evaluation indicates that the difference between the "fresh" and the air-exposed $Li_4Ti_5O_{12}$ is negligible in initial coulombic efficiency (91.3% *vs.* 91.1%) and reversible capacity (*ca.* 165.6 *vs.* 165.4 mAh g^{-1} at 0.1 C rate between 1.0 and 2.0 V *vs.* Li^+/Li). This might be due to the low content of Li_2CO_3 on the surface of $Li_4Ti_5O_{12}$ (0.143% *vs.* 0.417% mass loss between 450 and 800 °C in nitrogen obtained by TG–DSC analysis, see Fig. 5S). Since Li_2CO_3 is only observed on the surface of $Li_4Ti_5O_{12}$, its content is low (Fig. 5S), the structure of the bulk of $Li_4Ti_5O_{12}$ is hardly impacted (Fig. 1c), and, in particular, spinel $Li_4Ti_5O_{12}$ is well known for its cycling stability and rate performance, we did not try to evaluate its other electrochemical performances except for the above two issues.

The Li_2CO_3 on the air-exposed commercial $Li_4Ti_5O_{12}$ can be removed by heat-treating the latter at 800 °C for 2 h in air as is evidenced by FTIR, XRD and TEM tests (Figs. 6S–8S). However, we did not try to compare the electrochemical performances of commercial $Li_4Ti_5O_{12}$ before and after 800 °C annealing because such heat treatment changes its particle sizes and the impact of Li_2CO_3 formation on the electrochemical performance of $Li_4Ti_5O_{12}$ is actually not significant.

3.4. Reaction mechanism

The above results show that Li_2CO_3 will be formed on the surface of the spinel $Li_4Ti_5O_{12}$ stored in air. Both $LiTi_2O_4$ and $Li_4Ti_5O_{12}$ tend to be terminated with lithium atoms. Combining these facts, we may correlate the formation of Li_2CO_3 on air-exposed $Li_4Ti_5O_{12}$ with the reaction or absorption of CO_2 on $Li_4Ti_5O_{12}$, and propose the following reactions,

$$Li_4Ti_5O_{12} + 2CO_2 \rightarrow 2Li_2CO_3 + 5TiO_2, \quad \text{(a-1)}$$

followed by the lithium ion diffusion

$$TiO_2 + Li_4Ti_5O_{12}\,(\text{near } TiO_2) \rightarrow Li_xTiO_2 + Li_{4-x}Ti_5O_{12}. \quad \text{(a-2)}$$

Or the above reactions take place just as a one-step reaction

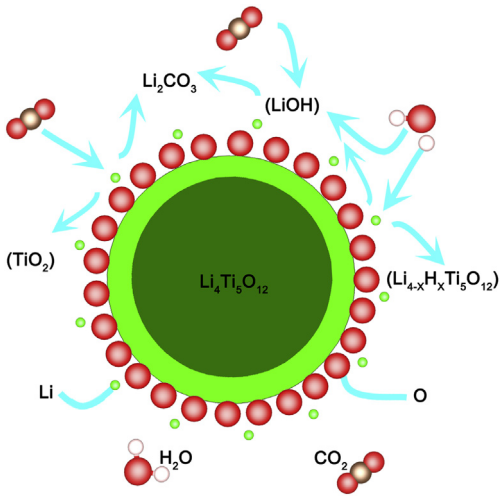

Fig. 7. A schematic illustration of the reactions between $Li_4Ti_5O_{12}$ and H_2O and CO_2 in air.

$$3Li_4Ti_5O_{12} + CO_2 \rightarrow Li_2CO_3 + 5/2\,(Li_xTiO_2 \cdot Li_{4-x}Ti_5O_{12}), \quad \text{(b)}$$

where Li_xTiO_2 and $Li_{4-x}Ti_5O_{12}$ form a complex in the surface area.

Another possible reaction is

$$Li_4Ti_5O_{12} + yCO_2 \rightarrow yLi_2CO_3 + Li_{4-2y}Ti_5O_{12-y}. \quad \text{(c)}$$

In this case, oxygen vacancy is produced. However, as the Ti–O bond is difficult to be broken (the formation energy for the Ti–O bond is 4.12 eV, as shown above), the probability for this reaction is very low.

Only the direct reactions between $Li_4Ti_5O_{12}$ and CO_2 are considered in the above. Due to the presence of H_2O in air, a proton-assisted H^+/Li^+ exchange reaction should also be considered. That is, the lithium-truncated surface of $Li_4Ti_5O_{12}$ is ready to adsorb H_2O and produces LiOH as well as $Li_{4-x}H_xTi_5O_{12}$. The LiOH then adsorbs CO_2 to form Li_2CO_3 in the surface area. This process is actually similar to what occurs in the acidic solutions [7]. Fig. 7 schemes the above proposed reactions.

However, due the amorphous feature of these products and the overlapping of the Ti–O vibrations below 900 cm^{-1} in the FTIR spectrum, only Li_2CO_3 can be well recognized at present. Further analysis is required to confirm the above proposed reaction products and the reaction mechanism.

4. Conclusions

Lithium-truncated surface is found beneficial in energy for $LiTi_2O_4$ and $Li_4Ti_5O_{12}$ according to first-principles calculations. This explains why the fresh $Li_4Ti_5O_{12}$ tends to absorb and react with H_2O and CO_2 in air and to have Li_2CO_3 formed on its surface. Although the Li_2CO_3 can be removed by heat-treatment, the impact of the formation and presence of some Li_2CO_3 on the electrochemical performances of commercial $Li_4Ti_5O_{12}$ is negligible. Therefore, air exposure at ambient temperature does not significantly influence the electrochemical performance of $Li_4Ti_5O_{12}$. This is attributed to the shielding effect of the TiO_6 layer to the inner layers once the outmost Li layer of $Li_4Ti_5O_{12}$ (and $LiTi_2O_4$) is removed (due to reactions with the outer environmental species, for example). However, this work will help to understand the surface structure features and throw light upon the storage/application of $Li_4Ti_5O_{12}$ and other electrode materials.

Acknowledgements

The authors appreciate the financial support of the National 973 Program of China (2009CB220100) and helpful discussion with Prof. Ouyang in Jiangxi Normal University.

Appendix A. Supplementary data

Supplementary data related to this article can be found at http://dx.doi.org/10.1016/j.jpowsour.2013.07.031.

References

[1] B. Scrosati, J. Garche, J. Power Sources 195 (2010) 2419–2430.
[2] T. Ohzuku, A. Ueda, N. Yamamoto, J. Electrochem. Soc. 142 (1995) 1431–1435.
[3] G.G. Amatucci, F. Badway, A. Du Pasquier, T. Zheng, J. Electrochem. Soc. 148 (2001) A930–A939.
[4] C.Y. Ouyang, Z.Y. Zhong, M.S. Lei, Electrochem. Commun. 9 (2007) 1107–1112.
[5] Z.Y. Zhong, C.Y. Ouyang, S.Q. Shi, M.S. Lei, ChemPhysChem 9 (2008) 2104–2108.
[6] Y.C. Chen, C.Y. Ouyang, L.J. Song, Z.L. Sun, Electrochim. Acta 56 (2011) 6084–6088.
[7] D.R. Simon, E.M. Kelder, M. Wagemaker, F.M. Mulder, J. Schoonman, Solid State Ionics 177 (2006) 2759–2768.
[8] M.Q. Snyder, W.J. DeSisto, C.P. Tripp, Appl. Surf. Sci. 253 (2007) 9336–9341.
[9] K. Matsumoto, R. Kyzuo, K. Takeya, A.J. Yamanaka, J. Power Sources 81–82 (1999) 558–561.
[10] K. Shizuka, C. Kiyohara, K. Shima, Y. Takeda, J. Power Sources 166 (2007) 233–238.
[11] G.V. Zhuang, G.Y. Chen, J. Shim, X.Y. Song, P.N. Ross, T.J. Richardson, J. Power Sources 134 (2004) 293–297.
[12] X. Xia, Z.X. Wang, L.Q. Chen, Electrochem. Commun. 10 (2008) 1442–1444.
[13] A. Boulant, J.F. Bardeau, A. Jouanneaux, J. Emery, J.Y. Buzare, O. Bohnke, Dalton Trans. 39 (2010) 3968–3975.
[14] P. Hohenberg, W. Kohn, Phys. Rev. 136 (1964) B864–B871.
[15] W. Kohn, J. Sham, Phys. Rev. 140 (1965) A1133–A1138.
[16] P.E. Blöchl, Phys. Rev. B 50 (1994) 17953–17979.
[17] J.P. Perdew, K. Burke, M. Ernzerhof, Phys. Rev. Lett. 77 (1996) 3865–3868.
[18] G. Kresse, J. Furthmüller, Phys. Rev. B 54 (1996) 11169–11186.
[19] G. Kresse, J. Furthmüller, Comput. Mater. Sci. 6 (1996) 15–50.
[20] O. Bengone, M. Alouani, P. Blöchl, J. Hugel, Phys. Rev. B 62 (2000) 16392–16401.
[21] A.I. Liechtenstein, V.I. Anisimov, J. Zaanen, Phys. Rev. B 52 (1995) R5467–R5470.
[22] S. Lutfalla, V. Shapovalov, A.T. Bell, J. Chem. Theory Comput. 7 (2011) 2218–2223.
[23] Z.P. Hu, H. Metiu, J. Phys. Chem. C 115 (2011) 5841–5845.
[24] G.C. Allen, M. Paul, Appl. Spectrosc. 49 (1995) 451–458.
[25] Z.X. Wang, X.J. Huang, L.Q. Chen, J. Electrochem. Soc. 150 (2003) A199–A208.
[26] Z.G. Lu, H.L. Chen, R. Robert, B.Y.X. Zhu, J.Q. Deng, L.J. Wu, C.Y. Chung, C.P. Grey, Chem. Mater. 23 (2011) 2848–2859.
[27] N. Ravet, M. Gauthier, K. Zaghib, J.B. Goodenough, A. Mauger, F. Gendron, C.M. Julien, Chem. Mater. 19 (2007) 2595–2602.
[28] G. Busca, V. Lorenzelli, Mater. Chem. 7 (1982) 89–126.
[29] J.C. Lavalley, Catal. Today 27 (1996) 377–401.
[30] E. Ferg, R.J. Gummow, A. de Kock, M.M. Thackeray, J. Electrochem. Soc. 141 (1994) L147–L150.